[AMERICAN JOURNAL OF SCIENCE, VOL. 282, OCTOBER, 1982, P. 1214-1231]

MECHANISM OF PYROXENE AND AMPHIBOLE WEATHERING II. OBSERVATIONS OF SOIL GRAINS*

ROBERT A. BERNER and JACQUES SCHOTT**

Department of Geology and Geophysics, Yale University,
New Haven, Connecticut 06520

ABSTRACT. *Studies of surface composition (via X-ray photoelectron spectroscopy and surface morphology (via scanning electron microscopy) have been conducted on partially weathered grains of hypersthene, augite, bronzite, diopside, and hornblende taken from soils developed on basic and ultrabasic rocks of the south and central Appalachians. Surface compositions of sonically cleaned grains indicate, on the average, some depletion of Ca and Mg relative to silica which agrees overall with the experimental results of Schott, Berner, and Sjöberg (1981); this shows that our short term experiments are applicable to long term weathering. Thicknesses of cation-depleted layers, from both the soil grain measurements and laboratory studies, are on the order of 5 to 20 Å and, thus, too thin to be considered as being diffusion-limiting in the classical sense. Also, no consistent evidence was found for the presence of an iron-rich and silica deficient, protective surface layer of ferric oxyhydroxide on the grains (although, in the outermost ~ 20 Å, Fe^{+2} in the silicate structure is oxidized to Fe^{+3}).*

Scanning electron microscope observations indicate that pyroxene and amphibole minerals dissolve during weathering by means of the formation, enlargement, and coalescence of distinctive lens-shaped etch pits. The etch pits are developed mainly on dislocation outcrops and are always aligned with their long axes parallel to the c-axis of the crystal. Their side-by-side coalescence results in the formation of sawtooth lined "cracks" and micro-caves whereas end-to-end coalescence results in a grooved and striated surface. Degree of etch pitting of coexisting pyroxenes and/or amphiboles can be used as a measure of relative weatherability.

Our results, along with those of Schott, Berner, and Sjöberg (1981), indicate that the rate of pyroxene and amphibole dissolution during weathering is controlled by surface chemical reaction and not by diffusion either through aqueous solution or through a protective layer on the mineral surface.

INTRODUCTION

The weathering of pyroxene and amphibole minerals constitutes one of the major processes in the geochemical cycles of magnesium and iron. From previous laboratory and field studies (Luce, Bartlett, and Parks, 1972; Siever and Woodford, 1979; Eggleton and Boland, 1981), it has been suggested that these and other ferromagnesian minerals undergo dissolution during weathering by the formation of a protective layer of altered composition on the surface of each crystal. This layer may consist of a Mg-depleted, protonated version of the underlying silicate (Luce, Bartlett,

* Paper presented at the Third International Conference on Water-Rock Interaction, Edmonton, Alberta, Canada, July 1980.

** Present address: Laboratoire de Minéralogie et Cristallographie, Université Paul-Sabatier, 31078 Toulouse Cedex, France

and Parks, 1972), a newly formed Mg-silicate of somewhat different structure type (Luce, Bartlett, and Parks, 1972; Eggleton and Boland, 1981) or a precipitate of ferric hydroxide (Siever and Woodford, 1979). In all cases the layer is assumed to be protective in the sense that diffusion of dissolved species to and from the unaltered primary mineral surface is inhibited by the layer. This means that the layer must be continuous, thick (greater than, say, 100 Å), relatively impervious, and must firmly adhere to the underlying mineral, as is found for the case of the protective corrosion of metals.

In the first paper of this series, Schott, Berner, and Sjöberg (1981) we showed, by way of laboratory experiments, that simulated dissolution during weathering (pH = 6, T = 20°C) results in the depletion of cations, relative to silica, on the surfaces of enstatite (Mg), diopside (Ca), and tremolite (Mg + Ca) but that this depletion is small and most likely confined to the outermost 5 to 15 Å. Other results indicated that the rate of dissolution of these minerals is controlled by surface reactions and not by diffusion, either in solution or through an altered surface layer. These results contradict the idea of a thick, protective surface layer. However, they need checking by observations of the surfaces of minerals that have undergone natural weathering.

In the present paper we further test the idea of a protective surface layer through observations of partially dissolved, or weathered, pyroxene and amphibole grains isolated from natural soils. For this purpose we employ scanning electron microscopy (SEM) for observation of surface morphology and X-ray photoelectron spectroscopy (XPS) for determination of surface composition. The latter technique (for example, see Petrovic, Berner, and Goldhaber, 1976) enables qualitative chemical analysis of the outermost few tens of angstroms of solid particles and is, thereby, well suited to testing for the existence of an hypothetical surface layer.

SOILS

The soils that we selected for study had to fulfill several criteria. First of all they had to contain abundant, partly dissolved pyroxenes or amphiboles. This meant that we had to find soils that formed from basic or ultrabasic igneous rocks or amphibole-containing metamorphic rocks. Secondly, the soils had to be developed, in situ, on geologically mapped rocks, or they couldn't be located. Third, the grain size had to be sufficiently large that individual minerals could be separated under a binocular microscope. This excluded sampling of, for example, basalts. Fourth, weathering had to be far enough along that the individual mineral grains had separated from one another but not so far along that the primary minerals were completely destroyed. Finally, regions affected by Pleistocene glaciation had to be excluded because of the problem that the soils might be developed on glacial till of heterogeneous mineralogical composition, rather than on the underlying bedrock.

Taking the above factors into consideration, we decided that the nearest regions to New Haven, Conn. that met all the criteria were the

central and southern Appalachians. Accordingly we collected soils from the following rock types and locations: Coffman Hill diabase, Bucks County, Pa. (augite and hypersthene); amphibolized pyroxenite, Hollofield Quarry, Baltimore County, Md. (hornblende); amphibolized peridotite, Ashe County, N.C. (hornblende); Websterite ultrabasic body, Webster, N.C. (bronzite and diopside). Both loose soils and unaltered original rocks were sampled at each locality. This was done to be able to compare altered with unaltered samples of the same mineral and to provide unweathered material for laboratory etching experiments.

METHODS

To remove obscuring clay from the surfaces of primary mineral grains all soil samples were suspended in water and treated with a high-energy ultrasonic cleaner. The resulting suspension of liberated fine-material was then decanted and removed along with any grains less than about 100 μm in size and flocculent soil organic matter. Efficiency of clay removal from grain surfaces was checked via SEM. Repeated soneration was necessary to dislodge all clay, and for two minerals, hypersthene and diopside, complete removal was unsuccessful (see below). For the Coffman Hill and Webster soils, the fine decanted material was allowed partially to settle and the <10 μm fraction collected for XPS and X-ray diffraction analysis. This fraction included minor fine fragments of pyroxenes, feldspars, et cetera as well as true clay minerals and iron oxides formed by weathering. Accordingly it is referred to loosely as "clay."

Sonically cleaned soil grains 0.5 to 3 mm in size were hand separated under a binocular microscope into monomineralic fractions. The exact mineralogical nature of each fraction was then ascertained via optical petrography and X-ray diffraction. Representative grains from each identified fraction were selected for further study and mounted on appropriate stubs for SEM and XPS analysis. In the case of hypersthene and diopside, separate subsamples were chosen to exhibit a range in surface clay content. Instruments used were an ETEC, Model U-1 Autoscan, for scanning electron microscopy, which is housed in the Peabody Museum of Yale University, and a Hewlett-Packard System Model 5950-A spectrometer, for X-ray photoelectron spectroscopy, which is housed in Yale's Department of Engineering and Applied Science.

In order to try to reproduce in the laboratory the dissolution features found via SEM, unweathered minerals were separated from the original rock from which each soil had formed. After crushing, freed monomineralic crystals were isolated under the binocular microscope, and then treated with a mixture of 5 percent HF + 12 percent HCl for various periods of time. The resulting etched material was then washed, dried, and examined under the scanning electron microscope. HCl was used to prevent the formation of insoluble fluoride precipitates on the mineral surfaces; by itself, it produced no discernible etch features.

XPS peaks used for studying mineral surface compositions were: Si_{2p}, Al_{2s}, Mg_{2s}, O_{1s}, $Ca_{2p\ 3/2}$, $Ca_{2p\ 5/2}$, and $Fe_{2p\ 3/2}$. In most cases individual peak areas, obtained by very slow scanning (2eV/sec, window = 20 eV),

were measured with a planimeter. Otherwise only peak heights were measured. In the case of O_{1s} small corrections for oxygen from mounting materials were made using blanks. All cationic composition data are normalized to Si_{2p} to remove variability due to sample size, counting statistics, et cetera. It should be kept in mind that peak ratios given are monotonically proportional but not equal to actual atomic ratios (for example, see Schott, Berner, and Sjöberg, 1981). Reproducibility, on separate samples of the same minerals, of ratios was ± 5 percent.

Additional subsamples of grains from each mineral fraction were ground to expose internal surfaces and then analyzed via XPS. In this way the interior composition of each mineral could be contrasted to that of its surface by comparing XPS peak ratios for ground and unground material respectively. In some cases the same grains previously analyzed via XPS were ground and re-analyzed giving a direct comparison.

Because it was impossible to obtain hypersthene and diopside grains completely free of obscuring surface clay, an extrapolation technique was adopted to determine clay-free surface composition for these minerals. This was done using data for aluminum. The aluminum content of the two minerals is much less than that in associated clays; thus, Al_{2s} peak height was used as a measure of surface clay content. Measured values of Al_{2s}/Si_{2p} for the grain interior were subtracted from surface Al_{2s}/Si_{2p} ratios as a crude representation of surface clay content. (Qualitative correlation between this parameter and degree of clay coating via very-high-magnification SEM was found.) The elemental ratios of interest (for example, Mg_{2s}/Si_{2p}) were then plotted versus ($Al_{2s}/Si_{2p\ surface} - Al_{2s}/Si_{2p\ interior}$), and the true surface value obtained by extrapolating to zero surface clay.

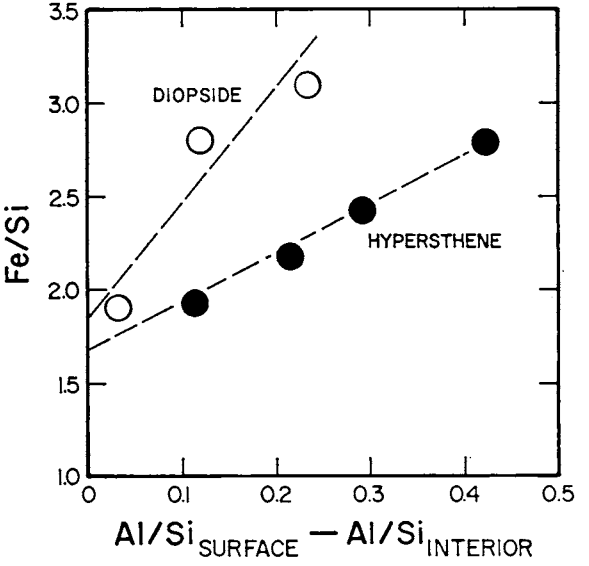

Fig. 1. Extrapolation plot for the determination of the clay-free surface Fe/Si XPS peak ratio of diopside and hypersthene. Peaks used are: Si_{2p}, Al_{2s}, and $Fe_{2p\ 3/2}$.

In the case of diopside the extrapolation was not too daring since the last measured points were close to the axis. As an aid the measured values of Al_{2s}/Si_{2p} for "clay" separated by soneration were also plotted and used in extrapolating. This is all shown in figures 1 and 2.

Besides peak intensity, we also looked at XPS peak positions, which record binding energies and, by small shifts, reflect changes in the state or environment of each element under study (for example, oxidation state, coordination number). (For a further discussion of peak shifts consult Carlson, 1975 or Koppelman and Dillard, 1979.) By using peak shifts one can spot the possible formation of new weathering products on mineral surfaces. For this purpose we examined positions for the interiors and surfaces of soil grains of the following peaks: Si_{2p}, Mg_{2s}, $Ca_{2p\ 3/2}$, $Fe_{2p\ 3/2}$, and O_{1s}. Reproducibility of measurements and resolution is approx. ± 0.2 eV. Because peak positions of Si_{2p}, using a gold standard, were found to be constant within measurement error for all minerals studied (in agreement with the results of Adams, Thomas, and Bancroft, 1972 and Carriere and others, 1977), we report our results for Ca, Mg, Fe, and O in terms of binding energies relative to Si_{2p}, (that is, $Mg_{2s} - Si_{2p}$) analogous to our results for peak areas which are also reported relative to Si_{2p}.

RESULTS

Surface morphology.—In general, removal of clay via sonification was extensive, and this allowed clear observation of the surfaces of the mineral grains. Scanning electron photomicrographs, selected from over 300 others to represent major morphological features, are shown in plates 1 to 7. The most obvious feature shown by the photos is an overall surface roughness reflecting laterally discontinuous dissolution over the grain surfaces. This is brought about by attack of the surfaces at points of excess energy,

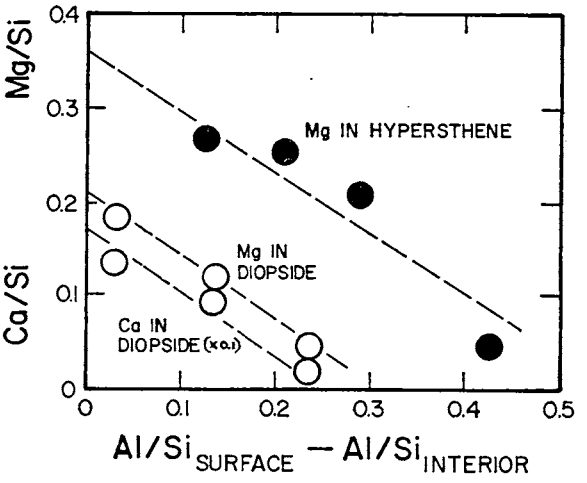

Fig. 2. Extrapolation plot for the determination of the clay-free surface Mg/Si and Ca/Si XPS peak ratios of diopside and hypersthene. Peaks used are: Si_{2p}, Al_{2s}, Mg_{2s}, and $Ca_{2p\ (3/2\ +\ 5/2)}$.

PLATE 1

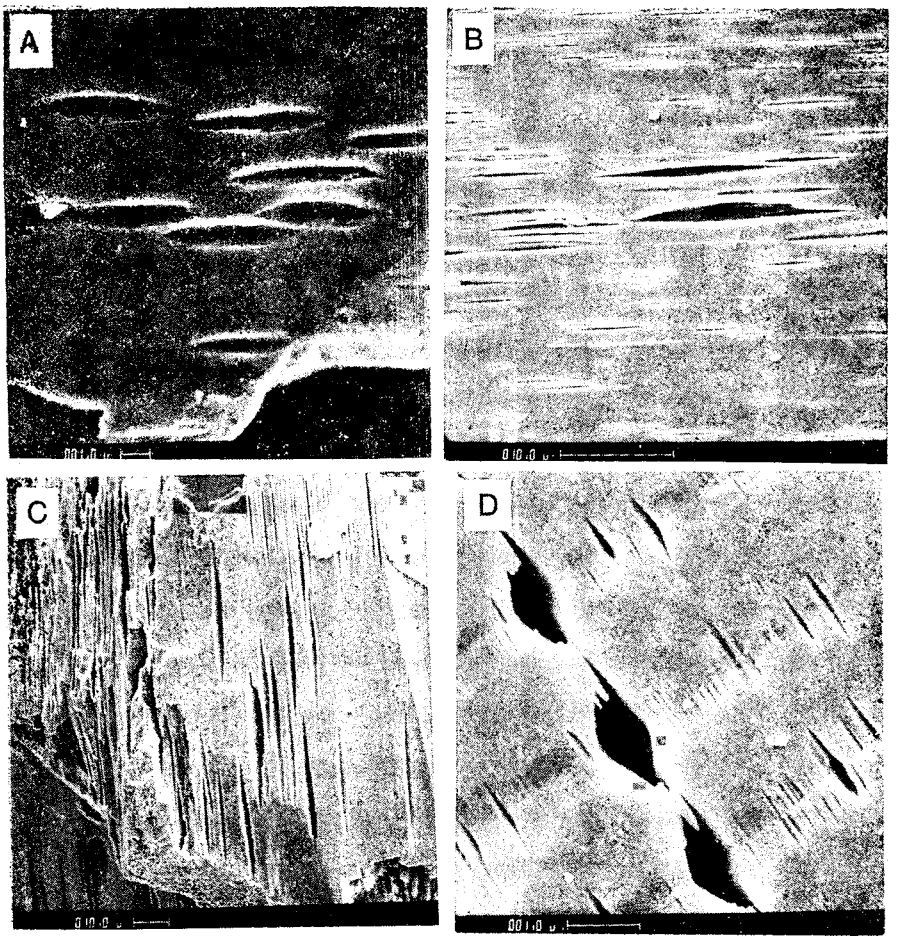

Lens-shaped etch pits (note parallelism): (A) hypersthene; (B) diopside; (C) hornblende; (D) augite (note side-by-side alignment along basal lamellae boundaries and compound etch pits resulting from lateral coalescence). (A) and (D) copyright 1980 by the American Association for the Advancement of Science (see Berner and others, 1980).

such as dislocation outcrops, resulting in the formation of characteristic, crystallographically controlled etch pits.

The basic etching unit found in all minerals from all soils, is the lens-shaped etch pit. This is illustrated, for hypersthene, augite, diopside, and hornblende, in plate 1. From studies of euhedral single crystals (for example, see pl. 4) the long axes of the etch pits were found always to parallel the c-axis of the crystal. Thus, pit orientation in anhedral grains can be used for crystallographic orientation. Side-by-side coalescence of pits, shown in plate 1-D, leads to the formation of wider compound pits, which can give a mistaken impression of individual pit shape. Normally single pits are quite long and narrow in cross section (for example, see

PLATE 2

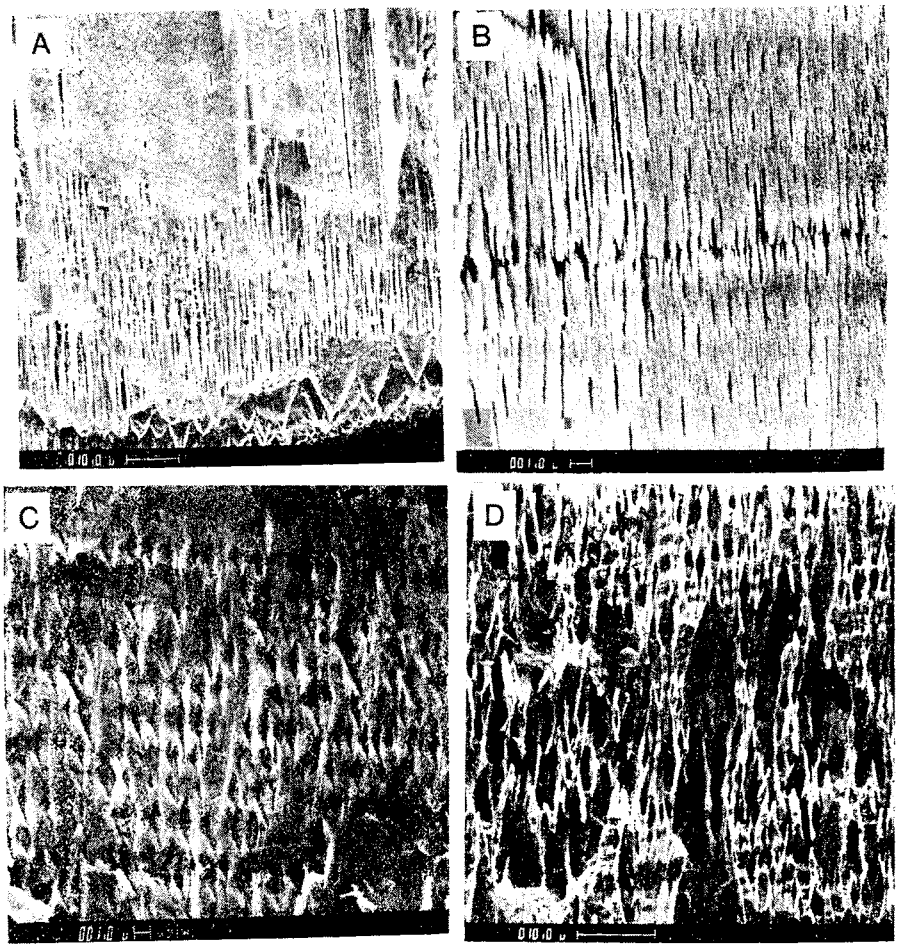

More-or-less homogeneous arrays of etch pits: (A) hypersthene; (B) hornblende; (C) augite; (D) augite.

pl. 1-C). Larger fields of view, showing many pits of varying width, are shown in plate 2.

Etch pits are often aligned, both end-to-end and side-by-side. End-to-end alignment, shown in plates 3-B and -D, can result in the formation of longitudinal grooves and striations which parallel the c-axis. Such grooves are shown, for a single crystal of diopside, in plate 4-A. Side-by-side alignment is more common (pl. 3-A, -C). This is especially true of augite where the alignment is most likely due to etching of dislocations at the boundaries of basal lamellae (pl. 1-D). (Lamellae boundaries should be sites of high dislocation density due to structural mismatch.)

Upon growth and coalescence of many side-by-side aligned etch pits, transverse sawtooth-lined microcracks can result (pls. 3-C, 5). The teeth

PLATE 3

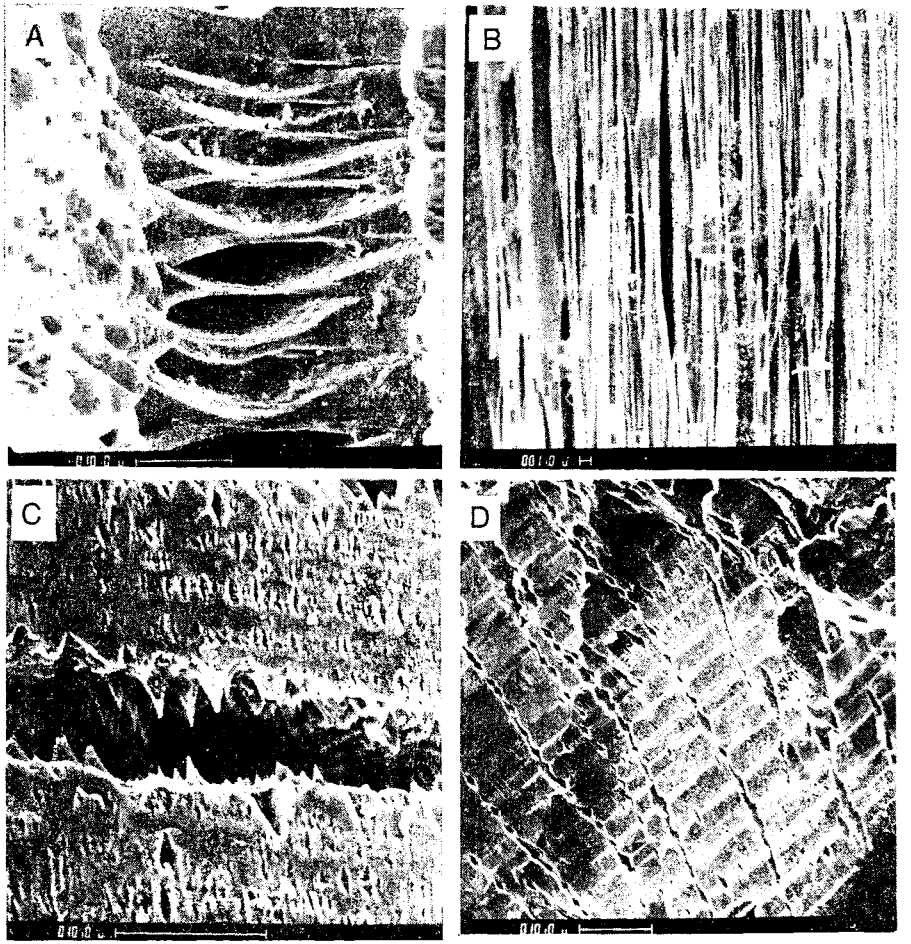

Etch pit alignment: (A) side-by-side alignment in hypersthene; (B) end-to-end alignment in diopside; (C) side-by-side alignment in augite (note formation of tooth-lined microcrack); (D) end-to-end alignment perpendicular to basal lamellae, in augite. (B) and (C) copyright 1980 by the American Association for the Advancement of Science (see Berner and others, 1980).

represent undissolved mineral between pits and are shown, in close up, in plate 5, A through D. Sometimes lateral coalescence of many pits results in features reminiscent of caves, as is shown in plate 5-A. (However, the "stalactites" are not a secondary precipitate like true stalactites.) The microcaves and microcracks are normally filled with clay-sized weathering product (pl. 5-C, -D) resulting, presumably, from the reprecipitation of material dissolved from the cave and crack walls. (The empty caves and cracks shown in the other photographs have undergone clay removal via ultrasonic cleaning.) Similar caves, cracks, and teeth are reported for partly dissolved hornblende and pyroxenes in sedimentary rocks (for

PLATE 4

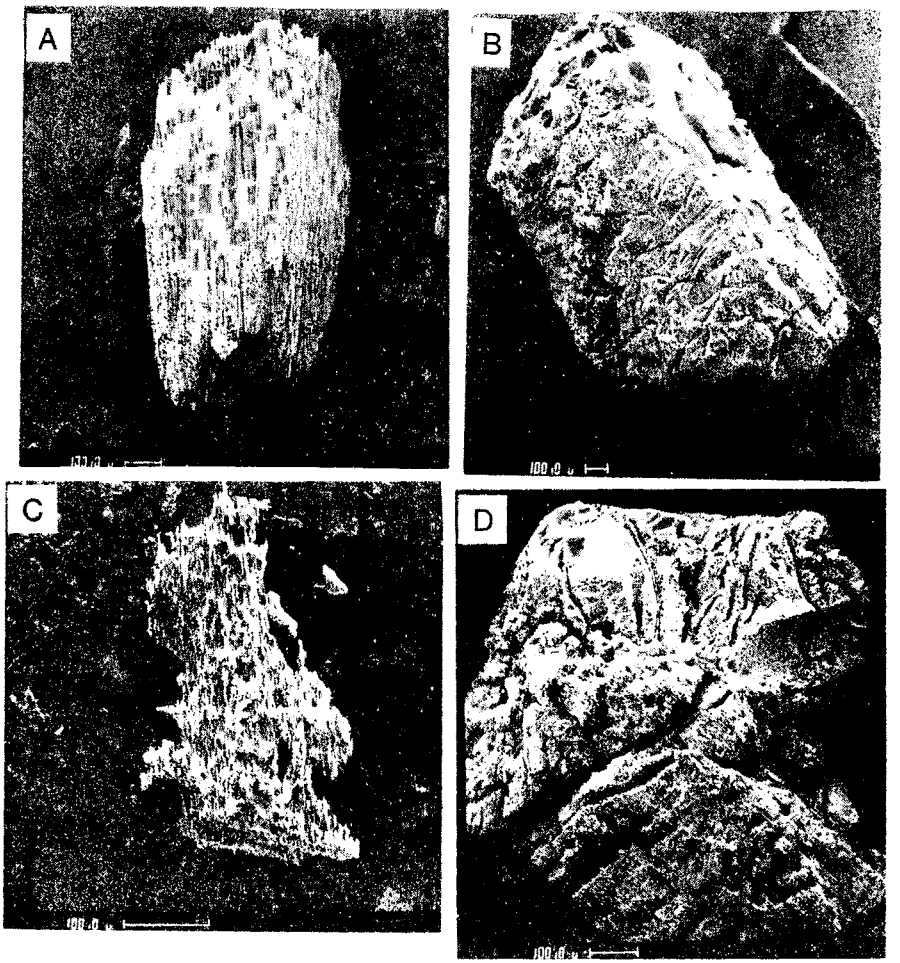

Large scale features resulting from etch pitting: (A) grooved and striated surface of a single crystal of diopside formed by end-to-end etch pit alignment; (B) transverse cracks on a single crystal of hypersthene resulting from side-by-side etch pit alignment; (C) fragile shell of augite single crystal as a result of extensive pitting; (D) compound grain consisting of single crystals of augite (lower portion of photo) and hypersthene (upper portion of photo). Note that the degree of pitting of the augite is greater than that of the co-existing hypersthene. (A) and (B) copyright 1980 by the American Association for the Advancement of Science (see Berner and others, 1980).

example, Walker, 1967, 1976; Waugh, 1978; Müller and Schwaighofer, 1979).

Upon prolonged weathering primary mineral grains may become very heavily pitted and result in the formation of fragile shells or ghosts. This is especially well shown in plate 4-C. Such shells should be easily disaggregated during erosive transport and, thus, may give rise to detrital pyroxene and amphibole grains which are much finer than those in the

PLATE 5

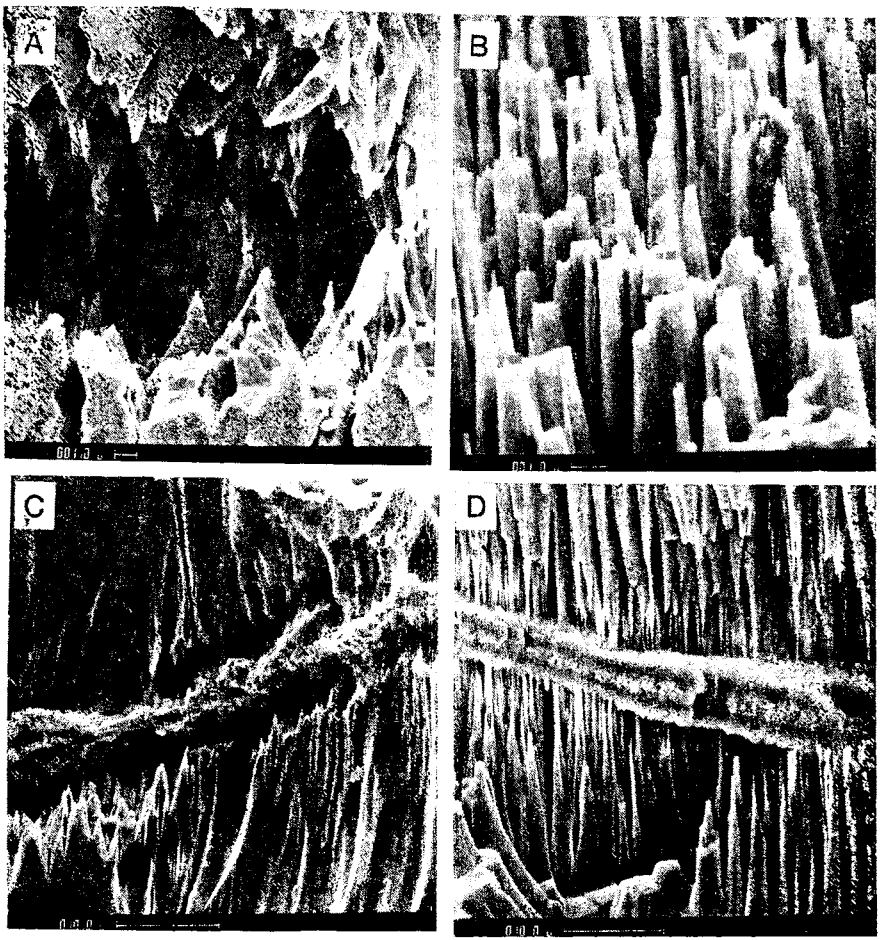

Microcaves, microcracks, and teeth produced by etch pit coalescence: (A) augite microcave; (B) hornblende teeth; (C) clay-filled microcrack in hypersthene; (D) clay-filled microcrack in hornblende. (A) and (B) copyright 1980 by the American Association for the Advancement of Science (see Berner and others, 1980).

original parent rock. Also, degree of pitting can be used to compare relative weathering rates of coexisting minerals. In plate 4-D is shown a compound grain consisting of a single crystal of augite joined to a single crystal of hypersthene. The augite is more heavily pitted indicating its greater weatherability.

Most of the etch features found in the soil grains could be duplicated by treating unweathered minerals from the soil host rocks with strong HF-HCl solution in the laboratory. Examples are illustrated in plates 6 and 7. Shown are lens shaped etch pits, side-by-side alignment, microcaves, teeth, et cetera. This shows that etching morphology is controlled primarily by the underlying crystal structure of the minerals. However,

PLATE 6

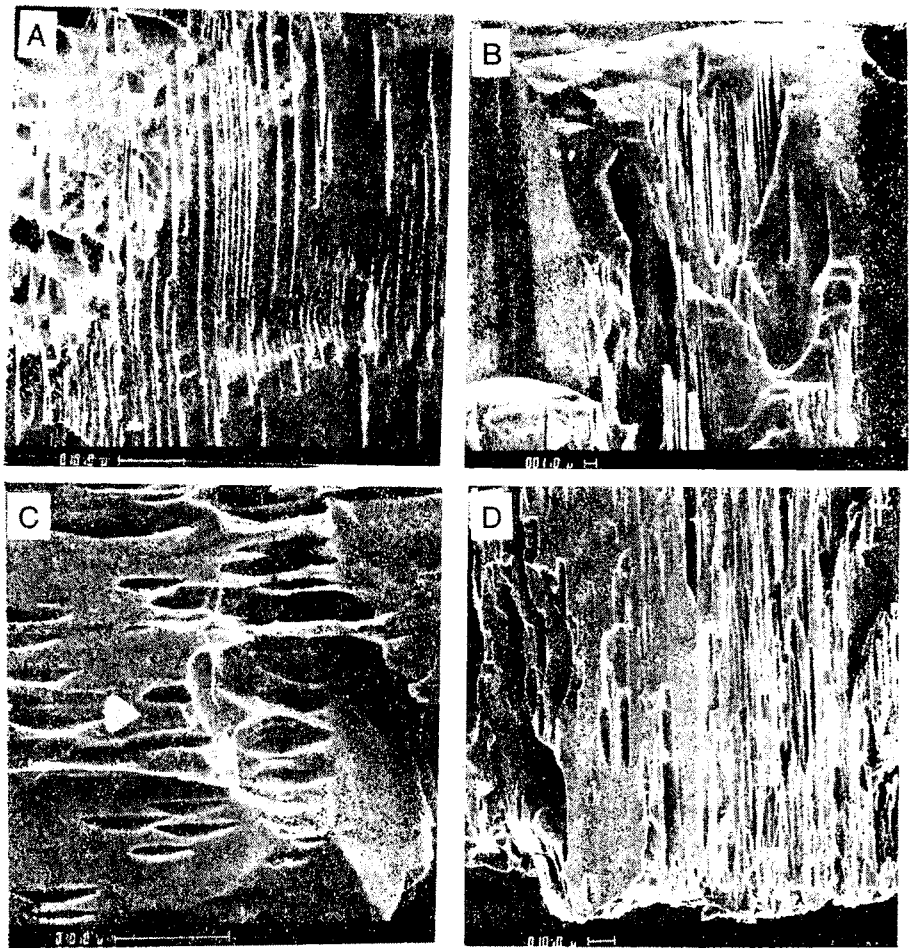

Etch pits produced in the laboratory by treating unweathered minerals with strong HF + HCl for various time periods: (A) hypersthene (24 hr etching); (B) augite (2 hr etching); (C) diopside (2 hr etching); (D) hornblende (2 hr etching).

duplication of the natural features was not as exact as found earlier for HF etching of feldspars (Berner and Holdren, 1979). This is seen in the photographs by etch pits that are more rectangular than lens-shaped (pl. 6-A, -D) and by blade-shaped, rather than pointed teeth (pl. 7-B). These differences suggest that etch pit shape is affected somewhat by the rate of etching and the nature of the etchant. In other words, slow weathering by soil acids on a geological time scale does not produce exactly the same features as produced by HF etching for a few hours in the laboratory.

Surface composition.—Results of surface compositions, determined via XPS, are shown in table 1. Included are values for "clay", separated

PLATE 7

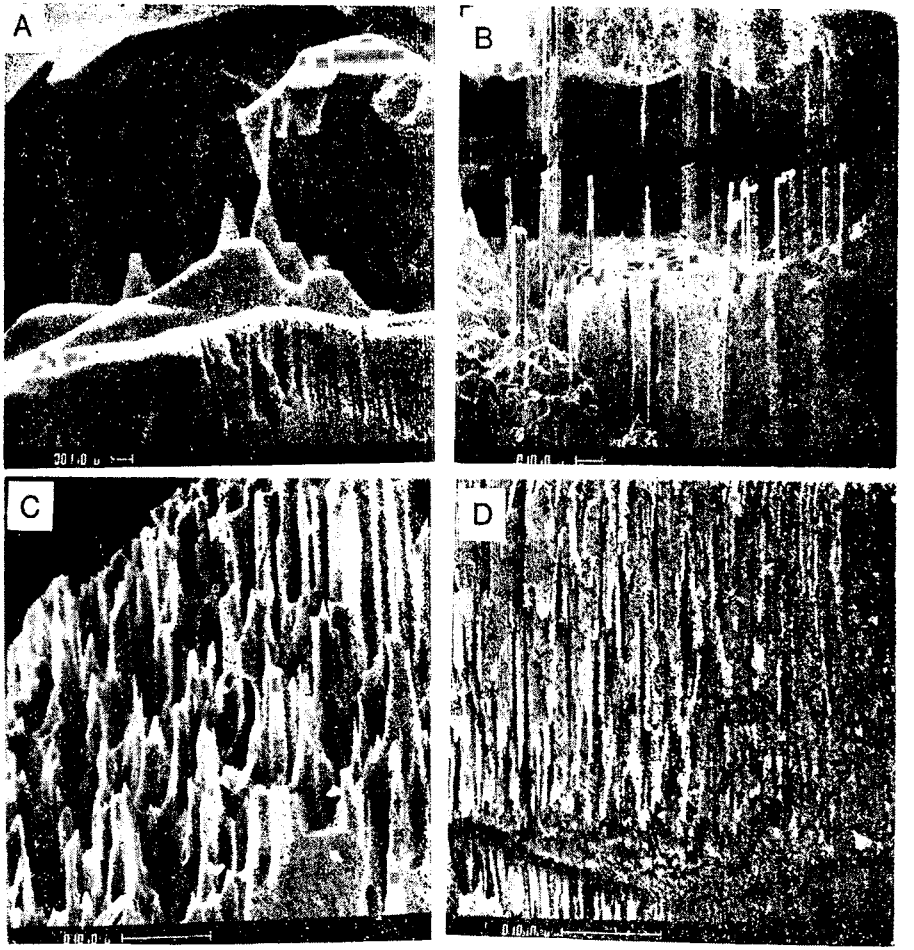

Features produced by etch pit coalescence as a result of treating unweathered minerals with strong HF + HCl for 2 hours: (A) microcave in augite (compare with fig. 5A); (B) microcave in diopside; (C) hornblende teeth (compare with fig. 5B); (D) longitudinal grooves in hornblende. (A) and (C) copyright 1980 by the American Association for the Advancement of Science (see Berner and others, 1980).

via soneration, from the same soils as the pyroxene and hornblende grains. The most obvious result shown in the table is that the outermost few tens of angstroms of the sonically cleaned primary mineral grains is far closer in composition to grain interiors than it is to associated clay weathering products. In other words, weathering does not produce a thick, tenacious, highly altered surface layer. What altered material that is produced (that is, "clay") is readily removed by soneration. The small degree of surface alteration, manifested by depletions in Mg and Ca relative to Si, is somewhat greater but still comparable to that found in our earlier experimental work (Schott, Berner, and Sjöberg, 1981). This

is shown in table 2. Apparently long term weathering in soils produces a surface roughly similar to that formed during only a few days dissolution in the laboratory.

Looked at in greater detail, the data of tables 1 and 2 show some interesting differences. In diopside, hornblende, and tremolite, surface depletions of Mg are somewhat less than they are for Ca, both in soils and in the laboratory dissolution experiments. This is in agreement with our earlier conclusion (Schott, Berner, and Sjöberg, 1981) that preferential loss of Ca relative to Mg occurs, because Ca occupies less strongly bonded M_2 sites in diopside and M_4 sites in tremolite and hornblende. Along these lines, the lack of surface depletion of *either* Mg or Ca in augite is puzzling. Perhaps the unusually high degree of etch pitting in this mineral has resulted in a totally unaltered surface.

Surface enrichment in Fe of ultrasonically cleaned grains is shown only for diopside. All other minerals exhibit surface values of Fe/Si essentially identical to their interiors. In addition, the O/Si ratio for the surfaces of bronzite and augite are essentially identical to their interiors. These Fe/Si and O/Si data show that precipitate layers of relatively pure ferric oxide or oxyhydroxide, as envisaged by Siever and Woodford (1979), may form on the surface but are readily removed by ultrasonic cleaning and, therefore, were not found in the present study. They are not adherent and, thus, not protective. This agrees with the results of our unpublished experimental work (Schott and Berner, in preparation).

Although iron does not, in general, accumulate at the grain surfaces, it does undergo a probable change in oxidation state. The data of table 3

TABLE 1

Relative composition, via XPS, of surfaces of ultrasonically cleaned soil grains as compared to their interiors. Also shown are surface compositions of associated "clay" removed by soneration. Values given refer to peak areas or heights and should not be confused with true atomic ratios. Values for Al/Si represent peak heights; all other data represent peak areas. Peaks used are: Si_{2p}, Al_{2s}, Mg_{2s}, O_{1s}, $Ca_{2p\ (3/2\ +\ 5/2)}$, $Fe_{2p\ 3/2}$.

Mineral	Portion	Mg/Si	Ca/Si	Fe/Si	O/Si	Al/Si
Bronzite	interior	0.48	<0.05	1.65	8.9	0.09
Bronzite	surface	0.38	<0.05	1.61	9.0	0.09
Diopside	interior	0.29	2.46	0.95	—	0.10
Diopside	surface	0.21*	1.70*	1.85*	—	0.10**
"Clay" associated with bronzite and diopside	surface	0.04	0.20	3.10	14.2	0.33
Hypersthene	interior	0.46	<0.05	2.00	—	0.05
Hypersthene	surface	0.36*	<0.05	1.70*	—	0.05**
Augite	interior	0.23	1.50	2.55	9.5	0.20
Augite	surface	0.21	1.49	2.44	9.4	0.17
"Clay" associated with hypersthene and augite	surface	0.05	0.20	2.80	12.3	0.48
Hornblende	interior	0.19	1.70	2.80	—	0.29
Hornblende	surface	0.13	0.90	3.10	—	0.32

* value determined by extrapolation (see figs. 1 and 2).

** value assumed for clay-free surface.

TABLE 2

Comparison of surface compositions, via XPS, of naturally (soil grains) and artificially (laboratory dissolution) weathered pyroxenes and amphiboles. Data for laboratory dissolution (pH = 6; T = 20°C) from Schott, Berner, and Sjöberg (1981). Element ratios based on Si_{2p}, Mg_{2s}, and $Ca_{2p\ (3/2\ +\ 5/2)}$.

Mineral	Surface Mg/Si / Interior Mg/Si	Surface Ca/Si / Interior Ca/Si
	Soil grains	
Bronzite	0.79	—
Hypersthene	0.82	—
Diopside	0.72	0.69
Augite	0.91	0.99
Hornblende	0.70	0.53
	Laboratory dissolution	
Enstatite	0.89	—
Diopside	1.00	0.85
Tremolite	0.91	0.84

TABLE 3

XPS binding energy peak maxima (in eV) for Mg_{2s}, $Ca_{2p\ 3/2}$, $Fe_{2p\ 3/2}$, and O_{1s} relative to Si_{2p} (energy differences) for surfaces and interiors of weathered mineral grains. $\Delta E = E_{(x\text{-}Si)surface} - E_{(x\text{-}Si)interior}$. Also shown are relative energies for Fe in associated clays. Measurement reproducibility = ± 0.2 eV.

Mineral		Relative binding energy				ΔE			
		Mg-Si	Ca-Si	Fe-Si	O-Si	Mg	Ca	Fe	O
Hypersthene	interior	−13.5	—	608.5	—	−0.2	—	1.1	—
	surface	−13.7	—	609.6	—				
Augite	interior	−13.7	244.6	608.7	428.9	0.1	0.2	1.0	−0.1
	surface	−13.6	244.8	609.7	428.8				
Diopside	interior	−13.6	245.0	608.5	—	0.0	−0.1	1.4	—
	surface	−13.6	244.9	609.9	—				
Bronzite	interior	−13.6	—	608.3	428.9	0.1	—	1.4	0.0
	surface	−13.5	—	609.7	428.9				
Hornblende	interior	−13.6	244.9	608.7	—	0.0	0.0	1.1	—
	surface	−13.6	244.9	609.8	—				
"Clay" associated with hypersthene and augite	surface	—	—	609.5	—	—	—	—	—
"Clay" associated with bronzite and diopside	surface	—	—	610.0	—	—	—	—	—

show that there are definite binding energy peak shifts for Fe, averaging about 1.2 eV, between surfaces and the interiors of sonically cleaned pyroxene and hornblende grains whereas no perceptible peak shifts (measurement error = ± 0.2 eV) occur for Ca and Mg. Comparison of (Fe-Si) relative peak energies for the grain surfaces with those for selected ferruginous minerals (table 4), indicate that the surface iron (Fe-Si = 609.7 ± 0.2 eV) is most likely present as hydrous ferric silicate (Fe-Si = 609.9 eV in nontronite) or hydrous ferric oxide (Fe-Si = 609.4 eV in goethite) and not as ferrous silicate (Fe-Si = 608.5 ± 0.3 eV) or anhydrous iron oxides (608.4 eV in hematite; 608.5 eV for ferric in magnetite). Comparisons of O-Si data indicate that oxygen in nontronite (428.9 eV) is more similar to that on the surfaces of augite (428.8 eV) and bronzite (428.9 eV) than is that in goethite (428.0 eV). In addition, the data of table 1 indicate O/Si peak area ratios on the surfaces of bronzite and augite which are essentially identical to those for their interiors. In other words, the surfaces of bronzite and augite are silicates, not oxides. Overall, taken together the Fe and O XPS data indicate the presence of Fe^{+3} on the outermost surface (few tens of angstroms) of the weathered, but sonically cleaned, mineral grains which is present as a silicate or hydroxysilicate and not as an oxide or oxyhydroxide.

In our earlier study (Schott, Berner, and Sjöberg, 1981) we found that during laboratory dissolution at moderate pH values (~ 6) the depletion of Ca relative to Si on the surfaces of diopside and tremolite occurred very early, in other words, during the first few hours. This was followed by congruent dissolution of Ca (and Mg) and unchanging surface composition for periods ranging up to 40 days. The explanation given for this was that a very thin, cation-depleted alteration zone, on the scale of a few atomic layers, (5-15 Å) forms initially on the surface and subsequently does not increase appreciably in thickness. As dissolution proceeds, preferential cation release at the inner surface of the zone is matched by total dissolution of cation-depleted silicate at its outer surface,

TABLE 4

XPS binding energy peak maxima (in eV) for $Fe_{2p\ 3/2}$ and O_{1s} relative to Si_{2p} (energy differences) for the interior portions (exposed by grinding) of some selected minerals (compare with table 3). Si_{2p} energies for magnetite, hematite, and goethite based on small amounts of magnesian olivine added as a standard. Measurement reproducibility ± 0.2 eV.

Mineral	Relative Binding Energy Fe-Si	O-Si
Olivine	608.8	428.8
Bronzite	608.3	428.9
Augite	608.7	428.9
Hornblende	608.7	428.9
Biotite	608.2	428.9
Nontronite	609.9	428.9
Magnetite	608.0*	—
Hematite	608.4	427.0
Goethite	609.4	428.0

* This peak is the sum of Fe^{+++} (608.5 eV) and Fe^{++} (607.1).

thereby maintaining constant thickness and constant composition. The outer surface dissolves readily because of the instability of the cation-depleted silicate material (for example, Luce, Bartlett, and Parks, 1972). This rapid dissolution prevents the zone from becoming thicker than a few atomic layers which means that it is too thin to be diffusion-limiting and protective.

The results of the present study show that Ca-depletion in soil grains of diopside and hornblende is somewhat more and in augite grains somewhat less than that found in the laboratory experiments. However, the differences are sufficiently small that calculated thicknesses of totally calcium-depleted surface layers are comparable to those found in the laboratory experiments; in other words only a few angstroms. This is shown, along with thicknesses of Mg-depleted layers, in table 5. (Two models are adopted, one for total depletion of the cation under consideration and the other for a linear increase with depth from zero to the cationic concentration in the unaltered mineral — for details of calculation consult Petrovic, Berner, and Goldhaber, 1976.) The data of table 5 demonstrate that prolonged weathering in the field does not produce appreciably thicker surface layers or zones of cation depletion, thus corroborating the idea that instability prevents such layers from becoming thicker. (As stated in our earlier paper, we still cannot clearly distinguish between our interpretation and the presence of a thicker layer which is only slightly depleted in cations. However, based on very high magnification SEM observations and solution chemical measurements during laboratory experiments, we can say that, if such a layer

TABLE 5

Comparison of calculated thicknesses of leached layers, via XPS, of naturally (soil grains) and artificially (laboratory dissolution) weathered pyroxenes and amphiboles. For method of thickness calculation and a description of laboratory results, consult Schott, Berner, and Sjöberg (1981).

		Thickness of the layer (Å)			
Mineral	pH	Mg total depletion	Mg linear increase with depth	Ca total depletion	Ca linear increase with depth
			Soil grains		
Bronzite	—	5	10	—	—
Hypersthene	—	4	8	—	—
Diopside	—	7	15	5	11
Augite	—	2	4	0	0
Hornblende	—	7	15	10	21
			Laboratory dissolution		
Enstatite	6	3	5	—	—
	1	12	25	—	—
Diopside	6	0	0	3	6
	1	6	11	8	16
Tremolite	6	1.5	3	3	6
	1	4	8	4	8

exists, it must be much less than 100 to 200 Å in thickness — see Schott, Berner, and Sjöberg, 1981.)

DISCUSSION AND CONCLUSIONS

In the present study no evidence was found for the existence of an appreciably thick protective layer of altered composition on the surfaces of pyroxene and amphibole grains undergoing weathering. Altered clay-sized material was present but could be removed from the grains by ultrasonic cleaning. This is not what would be expected if the clay were truly protective and strongly adherent, as is the case for protective corrosion layers on metals. (We found that such layers on samples of corroded steel and aluminum could not be removed by the same ultrasonic technique.) Surface compositions of ultrasonically cleaned grains were much closer to their interiors than to that of the removed clay-sized material. Some surface depletion of cations and oxidation of iron was found, but this could be accounted for in terms of altered surface layers only a few angstroms thick.

As stated earlier (Schott, Berner, and Sjöberg, 1981) an altered surface layer a few angstroms thick cannot be thought of as being diffusion limiting because the process of cation diffusion, as treated for example in the theory of Luce, Bartlett, and Parks (1972), requires greater thicknesses for its description. In addition, preferential attack of the mineral surfaces, with the consequent formation of etch pits, points to the importance of surface chemical processes in controlling rates of dissolution. Control of dissolution by laterally homogeneous diffusion through a protective surface layer predicts a general rounding of the surface which is not found.

These considerations lead to the conclusion, in agreement with our earlier results (Schott, Berner, and Sjöberg, 1981), that pyroxene and amphibole dissolution during weathering is a surface-reaction controlled process and not limited by bulk diffusion either in solution or through a protective surface layer. The mechanism of dissolution consists of H^+ ion attack, mainly at dislocation outcrops, on the grain surfaces resulting in etch pit formation and cation depletion, and this is accompanied by iron oxidation in the outermost atomic layer(s). The cation depletion does not penetrate inward with time, and as a result overall congruent dissolution of the minerals occurs. The products of dissolution, silica and cations, undergo precipitation to form clay minerals and iron oxides which may or may not crystallize in a topotactic relationship with the underlying primary silicates (Eggleton and Boland, 1981).

Formation of crystallographically controlled etch pits characterizes the weathering of feldspars as well as that of pyroxenes and amphiboles (Wilson, 1975; Tazaki, 1976; Keller, 1976; Eswaran and Bin, 1978; Nixon, 1979; Berner and Holdren, 1979). Many other minerals may also undergo extensive etch pit formation. Consequently, comparison of the degree of surface etching of coexisting minerals in a given soil may provide a useful tool for checking and revising the order of weatherability of minerals (such as that reported by Goldich, 1938) under different soil-forming conditions.

ACKNOWLEDGMENTS

Research was supported by National Science Foundation grants EAR 77-13098 and EAR 80-07815. We are indebted to M. A. Velbel and J. G. Dillard for helpful discussions, A. Pooley for SEM assistance, E. L. Sjöberg and M. D. Krom for aid in HF leaching experiments, and E. T. Cleaves, D. Neary, and M. A. Velbel for aid in the field collection of soils. Helpful reviews of the manuscript were provided by T. R. Walker and especially G. R. Holdren. Musical inspiration courtesy of E. Satie and H. Villa-Lobos.

REFERENCES

Adams, I., Thomas, J. M., and Bancroft, G. M., 1972, An ESCA study of silicate minerals: Earth Planetary Sci. Letters, v. 16, p. 429-432.

Berner, R. A., and Holdren, G. R., 1979, Mechanism of feldspar weathering II. Observations of feldspars from soils: Geochim. et Cosmochim. Acta, v. 43, p. 1173-1186.

Berner, R. A., Sjöberg, E. L., Velbel, M. A., and Krom, M. D., 1980, Dissolution of pyroxenes and amphiboles during weathering: Science, v. 207, p. 1205-1206.

Carlson, T. H., 1975, Photoelectron and Auger Spectroscopy: New York, Plenum Press.

Carriere, B., Deville, J. P., Brion, D., and Escard, J., 1977, X-ray photoelectron spectroscopy of silicon-oxygen compounds: Jour. Electron Spectrosc. Relat. Phenom., v. 10, p. 85-91.

Eggleton, R. A., and Boland, J. N., 1981, The weathering of enstatite: Clays and Clay Minerals, (in press).

Eswaran, H., and Bin, W. C., 1978, A study of a deep weathering profile on granite in peninsular Malaysia III. Alteration of feldspars: Soil Sci. Soc. America Jour., v. 42, p. 154-158.

Keller, W. D., 1976, Scan electron micrographs of kaolins collected from diverse environments of origin: Clays and Clay Minerals, v. 24, p. 107-113.

Koppelman, M. H., and Dillard, J. G., 1979, The application of X-ray photoelectron spectroscopy (XPS or ESCA) to the study of mineral surface chemistry, *in* Mortland, M. M., and Farmer, V. C., eds., Internat. Clay Conf. 1978: Amsterdam, Elsevier, p. 153-166.

Luce, R. W., Bartlett, R. W., and Parks, G. A., 1972, Dissolution kinetics of magnesium silicates: Geochim. et Cosmochim. Acta, v. 36, p. 35-50.

Müller, H. W., and Schwaighofer, B., 1979, Frittung oder tertiäre Verwitterung-Zur Frage der Rotfarbung in den tertiaren Liegendsedimenten des Basalts von Soob (Burgenland, Österreich) Verh. Geol. Wien, v. 2, p. 133-160.

Nixon, R. A., 1979, Differences in incongruent weathering of plagioclase and microcline: cation leaching vs. precipitates: Geology, v. 7, p. 221-224.

Petrović, R., Berner, R. A., and Goldhaber, M. B., 1976, Rate control in dissolution of alkali feldspar—I. Study of residual feldspar grains by X-ray photoelectron spectroscopy: Geochim. et Cosmochim. Acta, v. 40, p. 537-548.

Schott, J., Berner, R. A., and Sjöberg, E. L., 1981, Mechanism of pyroxene and amphibole weathering. I. Experimental studies of iron-free minerals: Geochim. et Cosmochim. Acta, v. 45, p. 2123-2135.

Siever, R., and Woodford, N., 1979, Dissolution kinetics and the weathering of mafic minerals: Geochim. et Cosmochim. Acta, v. 43, p. 717-724.

Tazaki, K., 1976, Scanning electron microscopic study of formation of gibbsite from plagioclase: Okayama Univ. Inst. for Thermal Spring Research Papers, no. 45, p. 11-24.

Walker, T. R., 1967, Formation of red beds in modern and ancient deserts: Geol. Soc. America Bull., v. 78, p. 353-358.

———— 1976, Diagenetic origin of continental redbeds, *in* Falke, H., ed., The Continental Permian in West Central, and South Europe (NATO Advanced Study Inst. Proc. Mainz, Germany), Dordrecht, Holland, D. Reidel Pub. Co., p. 240-282.

Waugh, B., 1978, Diagenesis in continental red beds as revealed by scanning electron microscopy, *in* Whalley, W. B., Scanning Electron Microscopy in the Study of Sediments: Geoabstracts, Norwich, England, p. 329-346.

Wilson, M. J., 1975, Chemical weathering of some primary rock-forming minerals: Soil Sci., v. 119, p. 349-355.